Electronic Supplementary Information

Tuning the Gate Opening Pressure of a Flexible Doubly Interpenetrated Metal-Organic Framework through Ligand Functionalization

Xiaodong Sun,[a] Yali Ma,[a] Jun Zhao,[b] DongSheng Li,[b] Guanghua Li,[a] Lirong Zhang*[a] and Yunling Liu*[a]

[a.] *State Key Laboratory of Inorganic Synthesis and Preparative Chemistry, College of Chemistry, Jilin University, Changchun 130012, P. R. China. E-mail: yunling@jlu.edu.cn; zlr@jlu.edu.cn*

[b.] *College of Materials and Chemical Engineering, Key Laboratory of Inorganic Nonmetallic Crystalline and Energy Conversion Material, China Three Gorges University, Yichang 443002, China*

S1. Calculation procedures of selectivity from IAST

The measured experimental data is excess loadings (q^{ex}) of the pure components C_2H_2, CO_2, CH_4, C_2H_6 and C_3H_8 for **JLU-Liu33F**, which should be converted to absolute loadings (q) firstly.

$$q = q^{ex} + \frac{pV_{pore}}{ZRT}$$

Here Z is the compressibility factor. The Peng-Robinson equation was used to estimate the value of compressibility factor to obtain the absolute loading, while the measure pore volume 0.36 $cm^3\ g^{-1}$ is also necessary.

The dual-site Langmuir-Freundlich equation is used for fitting the isotherm data at 298 K.

$$q = q_{m_1} \times \frac{b_1 \times p^{1/n_1}}{1 + b_1 \times p^{1/n_1}} + q_{m_2} \times \frac{b_2 \times p^{1/n_2}}{1 + b_2 \times p^{1/n_2}}$$

Here p is the pressure of the bulk gas at equilibrium with the adsorbed phase (kPa), q is the adsorbed amount per mass of adsorbent (mol kg^{-1}), q_{m1} and q_{m2} are the saturation capacities of sites 1 and 2 (mol kg^{-1}), b_1 and b_2 are the affinity coefficients of sites 1 and 2 (1/kPa), n_1 and n_2 are the deviations from an ideal homogeneous surface.

The selectivity of preferential adsorption of component 1 over component 2 in a mixture containing 1 and 2, perhaps in the presence of other components too, can be formally defined as

$$S = \frac{q_1/q_2}{p_1/p_2}$$

q_1 and q_2 are the absolute component loadings of the adsorbed phase in the mixture. These component loadings are also termed the uptake capacities. We calculate the values of q_1 and q_2 using the Ideal

Adsorbed Solution Theory (IAST) of Myers and Prausnitz.

S2. Supporting Figures

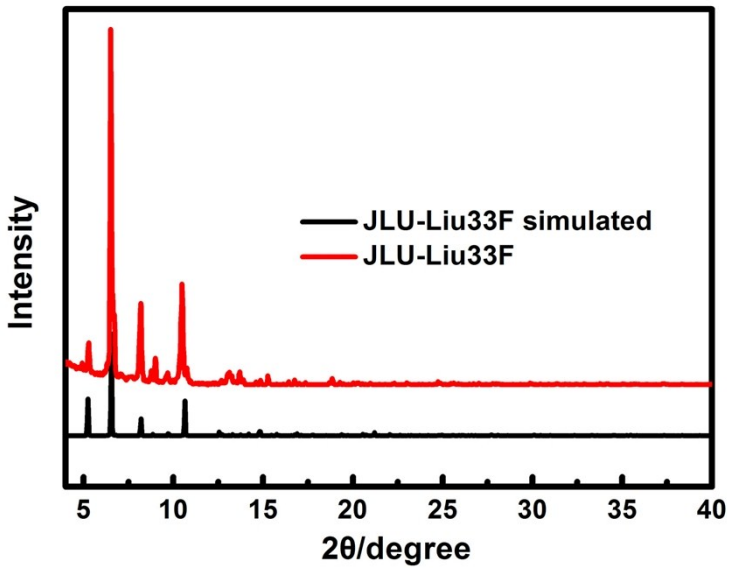

Fig. S1 PXRD patterns of simulated, as-synthesized sample for **JLU-Liu33F**

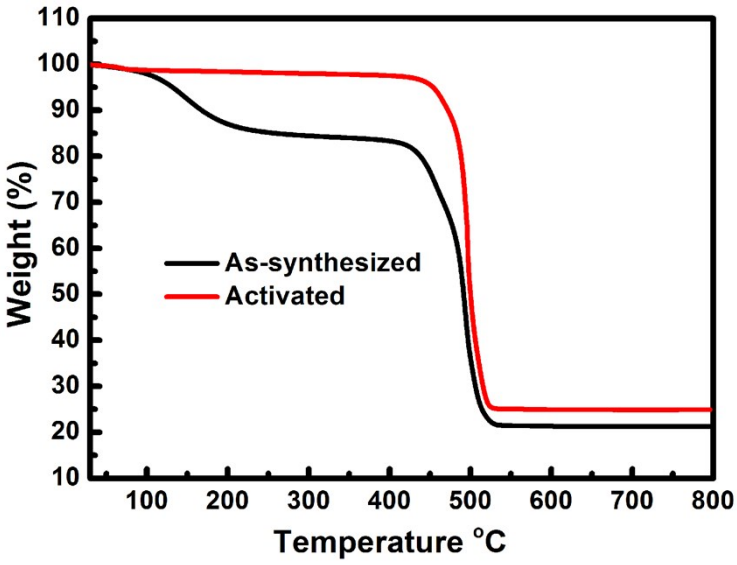

Fig. S2 TGA curves of **JLU-Liu33F** for the as-synthesized and activated samples.

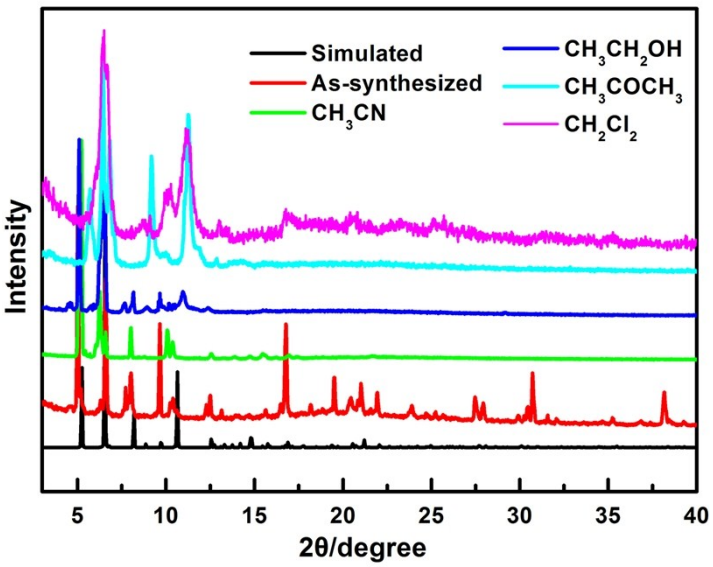

Fig. S3 PXRD patterns of **JLU-Liu33F** for simulated, as-synthesized and solvent-exchanged samples. **JLU-Liu33F** was stable in ethanol and acetonitrile and was relatively unstable in acetone and dichloromethane.

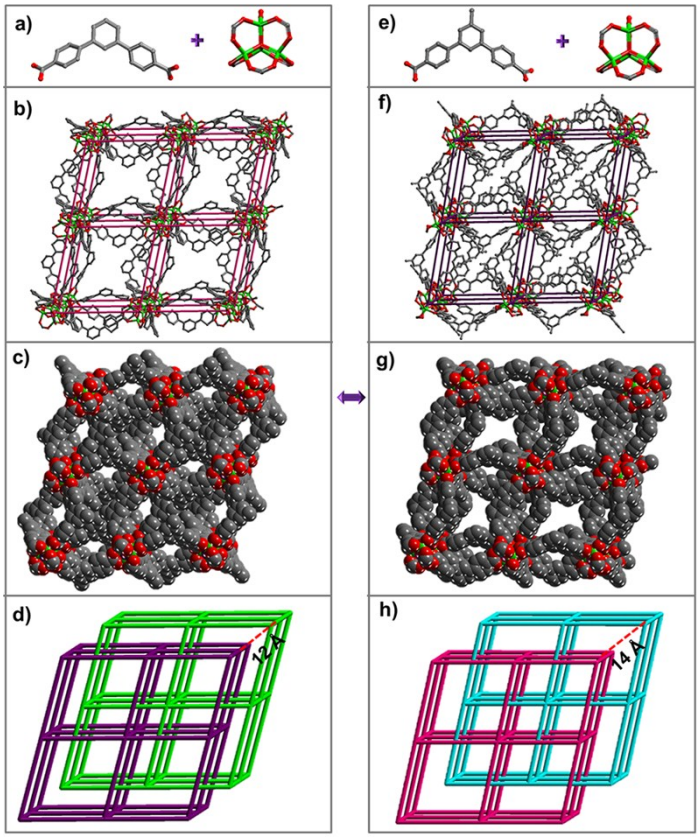

Fig. S4 Structure comparison of the two materials **JLU-Liu33** (left) and **JLU-Liu33F** (right): a) and e) The V-shaped ligands and Zn_4O clusters; b) and f) Single net of the framework; c) and g) Space-filling model of the channel for the single net along the [100] direction; d) and h) The difference of interpenetration degree.

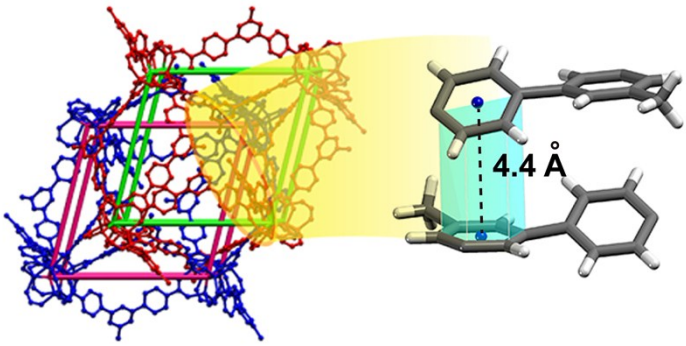

Fig. S5. The weak π…π interactions between the phenyl rings of H_2MDCPB ligands, which belong to two interpenetrated nets of **JLU-Liu33F**.

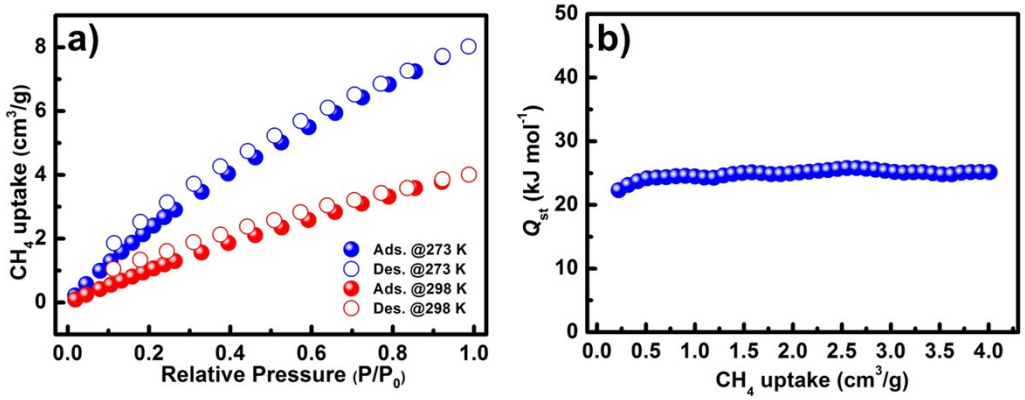

Fig. S6 (a) CH_4 adsorption isotherms for **JLU-Liu33F** at 273 and 298 K under 1 bar and (b) Q_{st} of CH_4 for **JLU-Liu33F**.

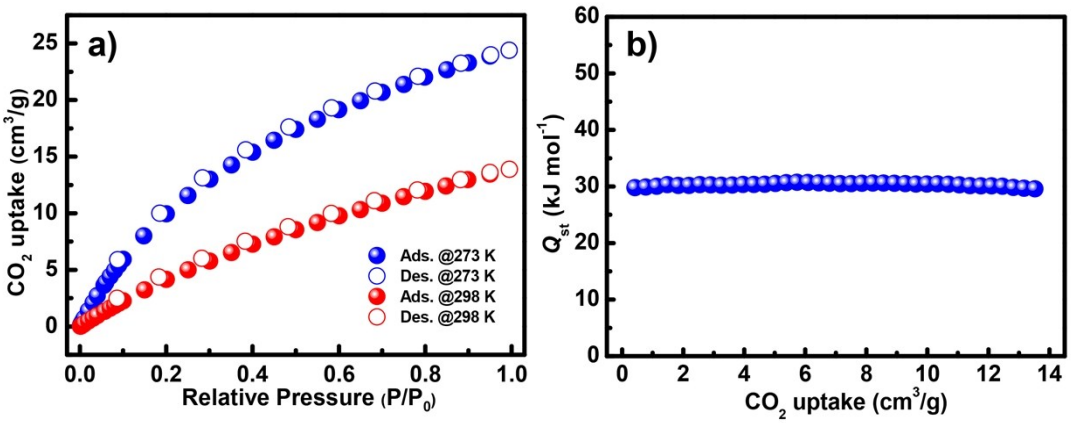

Fig. S7 (a) CO_2 adsorption isotherms for **JLU-Liu33F** at 273 and 298 K under 1 bar and (b) Q_{st} of CO_2 for **JLU-Liu33F**.

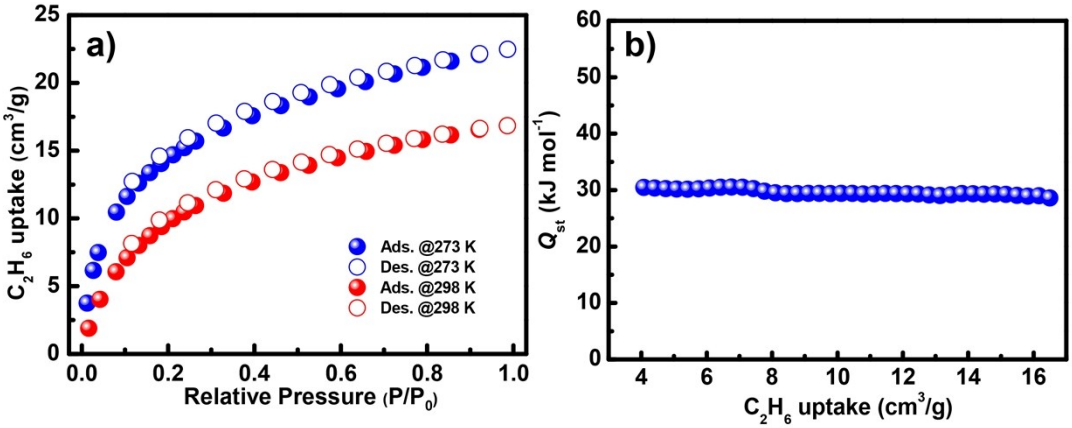

Fig. S8 (a) C_2H_6 adsorption isotherms for **JLU-Liu33F** at 273 and 298 K under 1 bar and (b) Q_{st} of C_2H_6 for **JLU-Liu33F**.

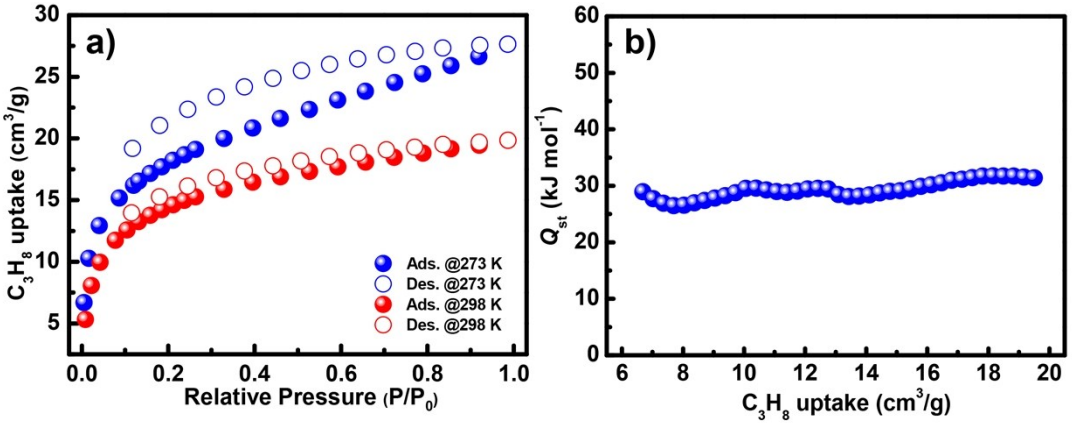

Fig. S9 (a) C_3H_8 adsorption isotherms for **JLU-Liu33F** at 273 and 298 K under 1 bar and (b) Q_{st} of C_3H_8 for **JLU-Liu33F**.

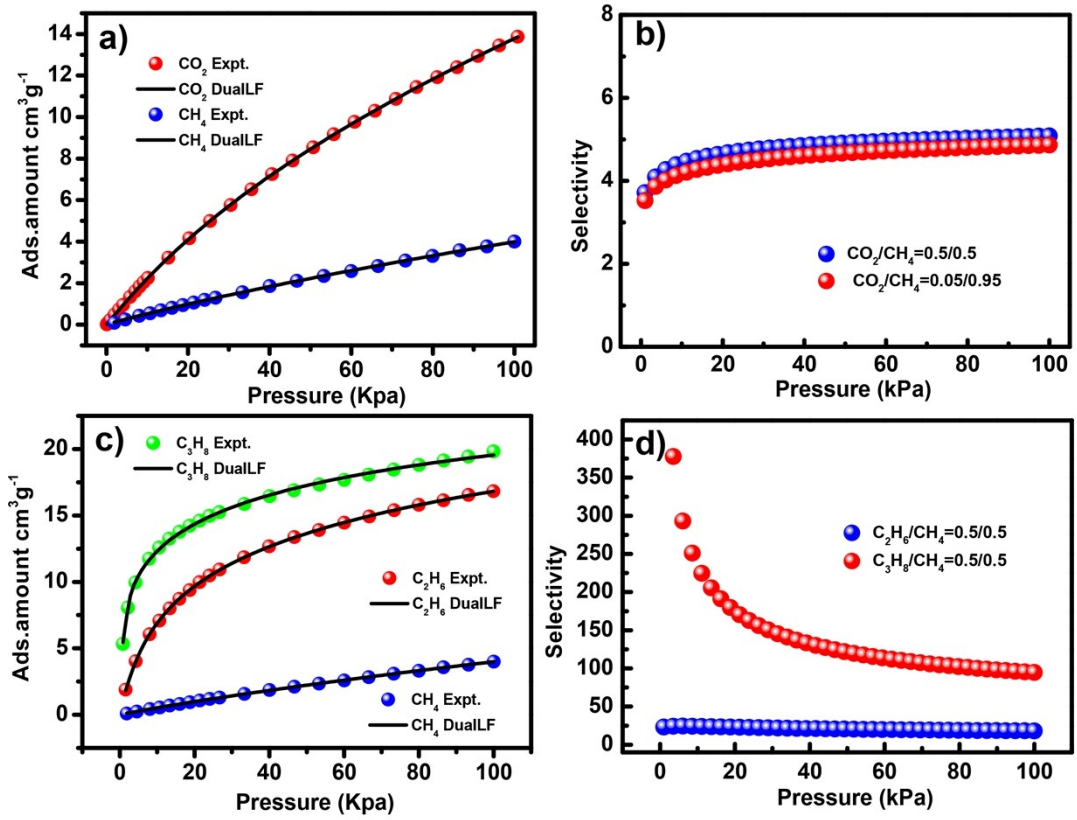

Fig. S10 CO_2, CH_4, C_2H_6 and C_3H_8 adsorption isotherms at 298 K along with the dual-site Langmuir Freundlich (DSLF) fits (a and c); gas mixture adsorption selectivity are predicted by IAST at 298 K and 100 kPa for **JLU-Liu33F** (b and d).

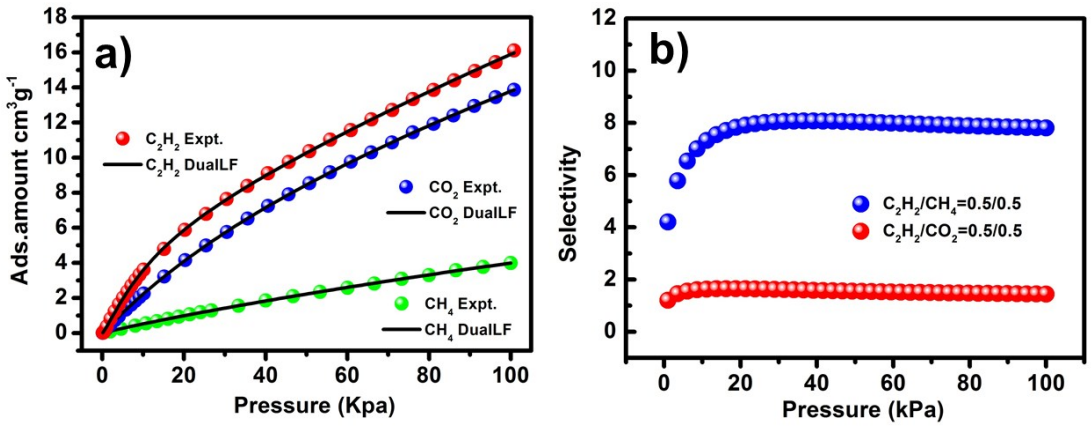

Fig. S11 (a) C_2H_2, CO_2 and CH_4 adsorption isotherms at 298 K along with the dual-site Langmuir-Freundlich (DSLF) fits; (b) C_2H_2/CH_4 and C_2H_2/CO_2 adsorption selectivity are calculated by IAST at 298 K and 1 bar for **JLU-Liu33F**.

S3. Supporting Tables

Table S1. Crystal data and structure refinement for **JLU-Liu33F**.

formula	$C_{138}H_{118}N_4O_{33}Zn_8$
formula weight	2883.32
temp (K)	293(2) K
wavelength (Å)	0.71073 Å
crystal system, space group	Trigonal, *R*3*c*
a (Å)	21.613(3)
b (Å)	21.613(3)
c (Å)	78.182(16)
V (Å^3)	31627(9)
Z, D_c (Mg/m^3)	6, 0.908
F(000)	8868
θ range (deg)	1.21 to 25.05°
reflns collected/unique	65434/12454
R_{int}	0.0580
data/restraints/params	12454/151/418
GOF on F^2	1.020
R_1, wR_2 (I>2σ(I))	R_1 = 0.0632, wR_2 = 0.1807
R_1, wR_2 (all data)	R_1 = 0.0994, wR_2 = 0.1997

After refining the crystal with the modern version refinement engine, the main CheckCIF A alerts have been solved. However, there still exists B alerts in the report. The B-level errors in the crystal data according to their checkCIF/PLATON report has been explained in the ESI: The bond length unrealistic is ascribed to weak CH···π interactions between the phenyl rings of H_2MDCPB ligands which belongs to two interpenetrated nets. The CH···π interactions lead to the deformation of the phenyl rings, so the C31-C34 bond length is longer. There also exists "Low bond precision on C-C Bonds" problems in the check report, but it will not influence the accuracy of the JLU-Liu33F structure.

Table S2. Selected bond lengths [Å] and angles [º] for **JLU-Liu33F**.

Zn(1)-O(1)	1.956(5)	O(6)-C(34)	1.242(16)
Zn(1)-O(5)	1.957(4)	O(7)-C(34)	1.283(15)
Zn(2)-O(5)	1.954(11)	O(8)-C(41)	1.128(11)
Zn(2)-O(11)	2.190(11)	O(9)-C(41)	1.562(10)
Zn(3)-O(10)	1.902(3)	C(1)-C(2)	1.3900
Zn(3)-O(6)	1.923(8)	C(1)-C(6)	1.3900
Zn(4)-O(10)	2.047(10)	C(1)-C(7)	1.518(6)
Zn(1)-O(3)#1	1.918(8)	C(2)-C(3)	1.3900
Zn(1)-O(2)#2	1.968(8)	C(7)-C(8)	1.3900
Zn(2)-O(11)#2	2.190(11)	C(7)-C(12)	1.3900
Zn(2)-O(11)#3	2.190(11)	C(8)-C(9)	1.3900
Zn(2)-O(4)#4	2.200(10)	C(10)-C(13)	1.452(10)
Zn(3)-O(7)#6	1.947(6)	O(1)-Zn(1)-O(5)	111.9(2)
Zn(4)-O(9)#10	1.887(5)	O(11)#2-Zn(2)-O(11)	36.5(4)
Zn(4)-O(9)#7	1.887(5)	O(5)-Zn(2)-O(4)#5	88.2(3)

O(1)-C(13)	1.273(9)	C(3)-C(4)-C(5)	120.0
O(2)-C(13)	1.273(10)	C(4)-C(5)-C(21)	119.0(6)
O(3)-C(20)	1.506(13)	C(8)-C(7)-C(12)	120.0
O(4)-C(20)	1.250(12)	C(8)-C(9)-C(10)	120.0

Symmetry transformations used to generate equivalent atoms:

#1 x-1/3,x-y+4/3,z-1/6 #2 -y+1,x-y+1,z #3 -x+y,-x+1,z #4 -y+5/3,-x+4/3,z-1/6 #5 -x+y-1/3,y-2/3,z-1/6 #6 -y+2,x-y+1,z #7 x+1/3,x-y+2/3,z+1/6 #8 -x+y+1,-x+2,z #9 -y+4/3,-x+5/3,z+1/6 #10 -x+y+4/3,y+2/3,z+1/6 #11 x+1/3,x-y+5/3,z+1/6 #12 x-1/3,x-y+1/3,z-1/6

Table S3. Gas adsorption data for **JLU-Liu33F**.

Gas	C_2H_2 (cm^3g^{-1})		CO_2 (cm^3g^{-1})		CH_4 (cm^3g^{-1})	
Temperature	273 K	298 K	273 K	298 K	273 K	298 K
Ads. amount	48	16	24	14	8	4
Gas	C_2H_6 (cm^3g^{-1})		C_3H_8 (cm^3g^{-1})		N_2 (cm^3g^{-1})	
Temperature	273 K	298 K	273 K	298 K	77 K	
Ads. amount	22	15	27	17	225	

Table S4. Comparison of several MOFs for their C_2H_2 uptake (273 K and 1 bar) and Q_{st} values.

Compound	**C_2H_2 uptake (273 K, cm^3 g^{-1})**	**Q_{st} (kJ mol^{-1})**	**Ref.**
SNNU-23	93	63	1
USTA-34b	N.A.	50	1
JLU-Liu33F	48	49	This work
SNNU-23	41	39	1
ZJNU-73	N.A.	33	2
ZJNU-74	N.A.	31	2
FJI-H8	277	32	3
NJU-Bai17	252	38	4
MFM-188	297	33	5
ZJU-12	241	29	6
MFM-300(V^{III})	182	29	7

N.A.; Not available

Table S5. A comparison with other MOFs which exhibits high selectivity for C_2H_2 over CH_4 under 1 bar.

Compound	Selectivity	Temperature (K)	Reference
Compound-1	229	273	8
ZJNU-81	48	278	9
ZJNU-82	39	278	9
ZJNU-83	34	278	9
ZJNU-58	47	278	10
ZJNU-59	28	278	10
JLU-Liu33F	57	273	This work
SNNU-22	36	273	1
SNNU-23	31	273	1
Zn-NH_2BTB-1-PIM	<31	273	1
CoTZB(INT)	<31	273	1
[InAg$(na)_4$]	17	273	11

REFERENCES

1. J. W. Zhang, M. C. Hu, S. N. Li, Y. C. Jiang and Q. G. Zhai, *Dalton Trans.*, 2017, **46**, 836-844.
2. F. Chen, D. Bai, D. Jiang, Y. Wang and Y. He, *Dalton Trans.*, 2017, **46**, 11469-11478.
3. J. Pang, F. Jiang, M. Wu, C. Liu, K. Su, W. Lu, D. Yuan and M. Hong, *Nat. Commun.*, 2015, **6**, 7575.
4. M. Zhang, B. Li, Y. Li, Q. Wang, W. Zhang, B. Chen, S. Li, Y. Pan, X. You and J. Bai, *Chem. Commun.*, 2016, **52**, 7241–7244.
5. F. Moreau, I. d. Silva, N. H. A. Smail, T. L. Easun, M. Savage, H. G. W. Godfrey, S. F. Parker, P. Manuel, S. Yang and M. Schröder, *Nat. Commun.*, 2016, **8**, 14085.
6. X. Duan, Y. Cui, Y. Yang and G. Qian, CrystEngComm, 2017, 19, 1464–1469.
7. Z. Lu, H. G. W. Godfrey, I. da Silva, Y. Cheng, M. Savage, P. Manuel, S. Rudic, A. J. Ramirez-Cuesta, S. Yang and M. Schroder, *Chem. Sci.*, 2018, **9**, 3401-3408.
8. H. R. Fu, Y. Zhao, Z. Zhou, X. G. Yang and L. F. Ma, *Dalton Trans.*, 2018, 47, 3725-3732.
9. M. He, Y. Wang, X. Gao, S. Li and Y. He, *Dalton Trans.*, 2018, **47**, 8983-8991.
10. Y. Wang, M. He, X. Gao, S. Li, S. Xiong, R. Krishna and Y. He, *ACS Appl. Mater. Interfaces*, 2018, **10**, 20559-20568.
11. Y. X. Tan, Y. P. He and J. Zhang, *RSC Adv.*, 2015, **5**, 7794-7797.